The effect of a depth-dependent bubble distribution on normal modes in the oceanic waveguide: quasistatic approximation.

The effect of a depth-dependent bubble distribution on normal modes in the oceanic waveguide: quasistatic approximation.

R.H.J. Grimshaw[a], K.R. Khusnutdinova[a] and L.A. Ostrovsky[b]

[a]Department of Mathematical Sciences,
Loughborough University, Loughborough LE11 3TU, UK

[b] Zel Technologies/ University of Colorado,
R/ET-O, 325 Broadway, Boulder, Colorado 80305, USA

Abstract

We consider the effect of a depth-dependent distribution of bubbles on internal and surface waves propagating horizontally in the oceanic waveguide. While our previous work was restricted to the case of a locally monodisperse mixture, in this paper we show that by using a quasistatic approximation (where attention is confined to those modes whose typical frequencies are much less than the natural frequency for bubble oscillations), we can extend that work to the case of more general discrete and continuous bubble distributions. The equations of motion are formulated in terms of the usual fluid variables and the void fraction of bubbles. Then, to leading order in the Boussinesq approximation, we obtain the usual equation for internal wave modes, but the value of the buoyancy frequency in the fluid is replaced by an effective buoyancy frequency which takes account of the bubble distribution. Two physical factors are shown to affect the buoyancy frequency in the mixture: the effective stratification due to the bubbles adds to the effect of stratification in the liquid, while the compressibility of the mixture due to the bubbles reduces the buoyancy frequency. Then, for a typical oceanic situation, the correction due to the first effect is shown to be more significant than the second correction. In accordance with existing observational evidence that the void fraction profile in the ocean decays exponentially with depth, we obtain an explicit description of the normal modes, and show that bubble distributions, when present, may considerably change the properties of the oceanic waveguide.

PACS numbers: 47.55.Hd, 47.55.Kf

Keywords: Normal modes, bubbles, internal waves

Corresponding author address: Dr. Karima R. Khusnutdinova,
Department of Mathematical Sciences, Loughborough University,
Loughborough LE11 3TU, UK
E-mail: K.Khusnutdinova@lboro.ac.uk

1 Introduction

The internal wave field constitutes a fundamental component of the ocean. For sufficiently large horizontal scales, it is customary to take account of the ocean's free surface and rigid bottom, and so reduce the study of internal waves to a normal mode structure with associated horizontal propagation features (e.g., LeBlond and Mysak 1978, Gill 1982, Miropol'sky 2001). It is well known that breaking surface waves inject bubbles into the ocean surface layer. Until recently, this feature has not been taken into account in determining the structure of normal modes. However, developments both in the observations of the structure of the bubble layer in the upper ocean (e.g., Thorpe 1982, Farmer, Vagle and Li 1999, Terrill and Melville 1999), and in the mechanics of multiphase media (e.g., Nigmatulin 1991), have allowed us to begin the consideration of the effect of bubbles on normal modes (Grimshaw and Khusnutdinova 2004 a,b).

According to Thorpe (1982), for winds exceeding 6.5 m s^{-1} there is a continuous bubble layer of variable thickness in the upper ocean, which may extend to a depth of several meters beneath the surface (see Farmer and Vagle 1989, Zedel and Farmer 1991, and Farmer et al. 1999). The observed bubble layer is highly structured, varies both spatially and temporally, and depends significantly on the wind speed. In general, there is a monotonic decrease in the bubble void fraction with increasing depth; the void fraction profile either decays exponentially, or may follow an inverse-square profile (Buckingham 1997). According to Farmer and Lemon (1984), the bubble concentration decreases exponentially with depth, with an e-folding scale of order 1 m, which depends on the wind speed. The distributions of the bubble radius peak at all depths, and decrease rapidly on either side of the peak, and also rapidly with depth (see, e.g., Thorpe 1984b, Farmer et al. 1999, Terrill and Melville 1999 and the references there). These observations have shown that bubbles with radii of approximately $50-100$ μm contribute most to the total void fraction (Farmer et al. 1999). A fuller review of the data gathered on the distributions of bubbles in the ocean can be found in our earlier work (Grimshaw and Khusnutdinova 2004 a,b).

Previously (Grimshaw and Khusnutdinova 2004 a,b) we have used a two-dimensional model of a dilute locally monodisperse mixture of an incompressible fluid with gas bubbles to model and study internal waves in the presence of a depth-dependent distribution of bubbles. Here, this work is extended to more realistic polydisperse mixtures, when, at fixed depth, there is either a discrete or a continuous distribution of bubbles. We restrict our attention to the low-frequency situation, where we assume that the characteristic frequencies of the normal modes are much less than the natural frequency for bubble oscillations. This assumption leads to a *quasistatic* approximation for the interaction of the bubbles with the fluid, in which only a pressure balance is needed and the actual radial oscillations of the bubbles are ignored. In this approximation, we can formulate the mathematical model in terms of the usual fluid variables, and only the total void fraction of bubbles, thus allowing us to consider more general bubble distributions. We then use a form of the Boussinesq approximation, to obtain an explicit analytical description of the normal modes (including the surface wave mode) for the important case of an exponentially decaying void fraction. Our results show that bubble distributions, when present, can have a profound effect on internal waves (but do not significantly affect the surface wave mode). In the conclusion we discuss some estimates of the bubble rise velocity and dissolution rate in relation to the assumptions and possible limitations of our present model.

2 Model formulation

We consider a polydisperse mixture of an incompressible fluid with small gas bubbles, each preserving their mass and spherical form. We first formulate the equations of motion for the case when there is a finite number of fractions of gas bubbles (characterized by their size in the basic state). We then generalize these equations to the case of a continuous bubble distribution.

We follow an approach developed in the mechanics of multiphase media (e.g., Nigmatulin 1991). The distances between the bubbles are supposed to be large enough to prevent collisions, and so the interaction between the bubbles is due only to pressure changes. The processes of bubble formation and destruction are not taken into account. It is assumed that bubbles move with the velocity of the fluid flow. The fluid phase is assumed to be incompressible, following the traditional approach towards studying internal waves (in the absence of bubbles). This is also justified by the great compressibility of bubbles compared to that of the surrounding fluid, and their small physical dimensions. The void fraction α_g is supposed to be small enough, $\alpha_g \ll 1$, so that the mass of the gas is neglected compared to the mass of the fluid. Thus, the mixture can be considered as a medium with density approximately equal to $\rho_l(1-\alpha_g)$. Here, surface tension and dissipative mechanisms are not taken into account (for a model accounting for these effects see Grimshaw and Khusnutdinova 2004a).

Under these assumptions the set of equations describing two-dimensional motion of the mixture takes the form

$$\rho\frac{du}{dt} + p_x = 0\,, \quad \rho\frac{dw}{dt} + p_z + \rho g = 0\,, \tag{1}$$

$$\frac{d\rho}{dt} + \rho(u_x + w_z) = 0\,, \quad \frac{dn_i}{dt} + n_i(u_x + w_z) = 0\,, \tag{2}$$

$$\rho_l\left(R_i\frac{d^2R_i}{dt^2} + \frac{3}{2}\left(\frac{dR_i}{dt}\right)^2\right) = p_{gi} - p\,, \tag{3}$$

$$\frac{d\rho_l}{dt} = 0\,, \;\; \rho = \rho_l(1-\alpha_g), \;\; \alpha_g = \frac{4}{3}\pi\sum_{i=1}^{N} n_i R_i^3\,, \tag{4}$$

$$\frac{d}{dt}(p_{gi}R_i^{3\kappa}) = 0\,. \tag{5}$$

Here p, ρ, u, w are pressure, density and velocity components of the mixture; ρ_l is the density of a pure fluid; p_{gi}, R_i, n_i are pressure, radius and number density of bubbles of the i-th fraction ($i = 1, 2, ..., N$); α_g is the total void fraction; κ is a polytropic exponent of a gas ($1 \le \kappa \le \gamma$, where γ is the adiabatic exponent) and $d/dt = \partial/\partial t + u\,\partial/\partial x + w\,\partial/\partial z$ is the material derivative with respect to time. This is essentially the Iordansky (1960), Kogarko (1961), Wijngaarden (1968) model, modified to take into account gravity, and the depth-dependence of the bubble layer (see also Nigmatulin 1991). For a fuller discussion of the model in a monodisperse case see Grimshaw and Khusnutdinova (2004 a, b).

Here, we consider in more detail the low-frequency situation, when the characteristic frequency of a wave is small compared to the natural frequency of bubble oscillations:

$$\omega \ll \omega_*.$$

This is appropriate when studying internal waves. In this case, the Rayleigh-Plesset equation (3) yields

$$p_{gi} = p, \quad \text{for all } i.$$

This approximation is called the *quasistatic* approximation, as it amounts to neglecting the actual radial oscillations of the bubbles. Then, from (5), we obtain

$$\frac{d}{dt}\ln(p^{1/\kappa}R_i^3) = 0, \quad \text{for all } i. \tag{6}$$

From (2) we have

$$\frac{d}{dt}\ln(n_i) = -(u_x + w_z), \quad \text{for all } i. \tag{7}$$

Adding equations (6) and (7) with a subsequent summation over all values of i yields

$$\frac{d}{dt}(p^{1/\kappa}\alpha_g) + p^{1/\kappa}\alpha_g(u_x + w_z) = 0. \tag{8}$$

From the second equation in (4) we find that

$$\frac{d\rho}{dt} = -\rho_l\frac{d\alpha_g}{dt} = -\frac{\rho}{1-\alpha_g}\frac{d\alpha_g}{dt}.$$

Therefore, we can exclude ρ_l from all equations. As a result, in the quasistatic approximation, we have the following reduced system of equations for the variables ρ, p, u, w, α_g:

$$\rho\frac{du}{dt} + p_x = 0, \quad \rho\frac{dw}{dt} + p_z + \rho g = 0, \tag{9}$$

$$\frac{1}{\rho}\frac{d\rho}{dt} = -\frac{1}{1-\alpha_g}\frac{d\alpha_g}{dt}, \quad u_x + w_z = \frac{1}{1-\alpha_g}\frac{d\alpha_g}{dt}, \tag{10}$$

$$\frac{d}{dt}(p^{1/\kappa}\alpha_g) + p^{1/\kappa}\alpha_g(u_x + w_z) = 0. \tag{11}$$

This equation set has the same form as that for a monodisperse mixture in this present quasistatic approximation.

Now let us generalize the previous model to the case of a continuous distribution of bubbles. We assume that bubbles are distributed by their size in the basic state, and $c(R_0, z)dR_0$ is the number density of bubbles with radii in the interval from R_0 to $R_0 + dR_0$. Then, the void fraction of bubbles in the basic state is

$$\alpha_{g0}(z) = \int_{R_{0min}}^{R_{0max}} \frac{4}{3}\pi R_0^3 c(R_0, z)dR_0.$$

In the current state, we define the void fraction as

$$\alpha_g = \int_{R_{0min}}^{R_{0max}} \frac{4}{3}\pi R(R_0, t, x, z)^3 c(R_0, t, x, z)dR_0,$$

and require that the number of bubbles, which in the basic state have the radii in the interval from R_0 to $R_0 + dR_0$ is preserved:

$$\frac{dc}{dt} + c(u_x + w_z) = 0. \tag{12}$$

The current radius R should satisfy the Rayleigh-Plesset equation. Here, again, we restrict our attention to the low-frequency quasistatic limit. Therefore, locally, $p_g = p$, and

$$\frac{d}{dt}(p^{1/\kappa}R^3) = 0. \tag{13}$$

Multiplying (13) by $\frac{4}{3}\pi c(R_0, t, x, z)$ and integrating with respect to R_0, we obtain

$$\frac{d}{dt}\left(p^{1/\kappa}\int_{R_{0min}}^{R_{0max}}\frac{4}{3}\pi R^3 c\; dR_0\right) - p^{1/\kappa}\int_{R_{0min}}^{R_{0max}}\frac{4}{3}\pi R^3\frac{dc}{dt}\; dR_0 = 0,$$

which leads, on using (12), to equation (8). Here we have assumed that R_{0max}, R_{0min} are constants. Thus, for the continuous distribution of bubbles, in the quasistatic approximation, we again have the system of equations (9) - (11).

Finally let us note, that equations for the monodisperse mixture can be obtained by setting

$$c(R_0, t, x, z) = n(t, x, z)\delta(R_0 - a),$$

where a is the radius of bubbles in the basic state. Indeed, in this case,

$$\alpha_g = \int_{R_{0min}}^{R_{0max}}\frac{4}{3}\pi R^3 c\; dR_0 = \frac{4}{3}\pi R^3 n,$$

where R is the current radius of the bubbles. For a finite number of fractions,

$$c(R_0, t, x, z) = \sum_{i=1}^{N} n_i(t, x, z)\delta(R_0 - a_i), \quad i = 1, 2, ..., N.$$

3 Boussinesq approximation

Let us introduce the dimensionless variables

$$\tilde{\rho} = \frac{\rho}{\rho_*}, \quad \tilde{p} = \frac{p}{\rho_* g h_*}, \quad \tilde{u} = \frac{u}{h_* N_*}, \quad \tilde{w} = \frac{w}{h_* N_*}, \quad \tilde{\alpha}_g = \frac{\alpha_g}{\sigma\alpha_*},$$
$$\tilde{t} = N_* t, \quad \tilde{x} = \frac{x}{h_*}, \quad \tilde{z} = \frac{z}{h_*},$$

where h_* is a typical depth of the stratified layer, N_* is a typical value of the buoyancy frequency in the mixture, ρ_* is a typical density value, and $\sigma\alpha_*$ is a typical value of the void fraction. Here, $\sigma = h_* N_*^2/g$ is the Boussinesq parameter, which is very small in typical oceanic conditions, and so will seek a reduced form of the model valid when $\sigma \ll 1$.

Then, equations (9) - (11) assume the following non-dimensional form (the tilde superscripts are omitted):

$$\rho\frac{du}{dt} + \frac{1}{\sigma}p_x = 0, \tag{14}$$

$$\rho\frac{dw}{dt} + \frac{1}{\sigma}(p_z + \rho) = 0, \tag{15}$$

$$\frac{1}{\rho}\frac{d\rho}{dt} = -\frac{\sigma\alpha_*}{1 - \sigma\alpha_*\alpha_g}\frac{d\alpha_g}{dt}, \tag{16}$$

$$u_x + w_z = \frac{\sigma\alpha_*}{1 - \sigma\alpha_*\alpha_g}\frac{d\alpha_g}{dt}, \tag{17}$$

$$\frac{d}{dt}(p^{1/\kappa}\alpha_g) + p^{1/\kappa}\alpha_g(u_x + w_z) = 0. \tag{18}$$

We will suppose that in the basic state the mixture has density $\rho_0(z)$, a corresponding pressure $p_0(z)$ (satisfying $p_{0z} = -\rho_0$), and that there is no shear flow, $u_0 = w_0 = 0$. The void fraction of bubbles in the basic state is also assumed to be a function of depth only:

$\alpha_g = \alpha_{g0}(z)$. Here, we take into consideration only the vertical variability of the bubble layer and do not consider the horizontal spatial variations of its thickness, which in reality is a significant feature of the upper ocean. However, including such horizontal variability in the basic state leads to forbidding technical difficulties in analysing these equations, and so, as a first step, we focus here solely on the effects due to the vertical variability of the bubble layer.

We now perturb this basic state, assuming that

$$\rho = \rho_0(z) + \sigma\tilde{\rho}, \quad p = p_0(z) + \sigma\tilde{p}, \quad u = \tilde{u}, \quad w = \tilde{w},$$
$$\alpha_g = \alpha_{g0}(z) + \tilde{\alpha}_g.$$

Linearizing equations (14) - (18) about the basic state, we obtain, after omitting the tilde superscript,

$$\rho_0 u_t + p_x = 0, \tag{19}$$
$$\rho_0 w_t + p_z + \rho = 0, \tag{20}$$
$$\sigma\rho_t + \rho_{0z}w = -\frac{\rho_0\sigma\alpha_*}{1-\sigma\alpha_*\alpha_{g0}}(\alpha_{gt} + \alpha_{g0z}w), \tag{21}$$
$$u_x + w_z = \frac{\sigma\alpha_*}{1-\sigma\alpha_*\alpha_{g0}}(\alpha_{gt} + \alpha_{g0z}w), \tag{22}$$
$$\sigma p_t + \frac{\kappa p_0}{\alpha_{g0}}\alpha_{gt} + (\kappa p_0\frac{\alpha_{g0z}}{\alpha_{g0}} + p_{0z})w + \kappa p_0(u_x + w_z) = 0. \tag{23}$$

Note that here ρ_{0z} is $O(\sigma)$ so that all terms in (21) are of the same order.

This system can be reduced to just two equations for the variables w and α_g. The horizontal velocity u can be eliminated by taking the time derivative of (22) and using the horizontal momentum equation (19). This results in

$$\frac{1}{\rho_0}p_{xx} = w_{zt} - \frac{\sigma\alpha_*}{1-\sigma\alpha_*\alpha_{g0}}(\alpha_{gtt} + \alpha_{g0z}w_t). \tag{24}$$

We then take the time derivative of the vertical momentum equation (20) and use (21) to eliminate ρ, which leads to

$$\frac{1}{\rho_0}p_{zt} = -w_{tt} + \left(\frac{1}{\sigma}\frac{\rho_{0z}}{\rho_0} + \frac{\alpha_*\alpha_{g0z}}{1-\sigma\alpha_*\alpha_{g0}}\right)w + \frac{\alpha_*}{1-\sigma\alpha_*\alpha_{g0}}\alpha_{gt}. \tag{25}$$

Then, the pressure p can be eliminated by taking the second derivative of (25) with respect to x and second derivative of (24) with respect to z and t. In the usual Boussinesq approximation (neglecting $(1/\rho_0)_z\, p_{xxt}$ term) this gives

$$\frac{\partial^2}{\partial t^2}(w_{xx} + w_{zz}) - \left(\frac{1}{\sigma}\frac{\rho_{0z}}{\rho_0} + \frac{\alpha_*\alpha_{g0z}}{1-\sigma\alpha_*\alpha_{g0}}\right)w_{xx}$$
$$-\frac{\alpha_*}{1-\sigma\alpha_*\alpha_{g0}}\alpha_{gtxx} - \left[\frac{\sigma\alpha_*}{1-\sigma\alpha_*\alpha_{g0}}(\alpha_{gttt} + \alpha_{g0z}w_{tt})\right]_z = 0. \tag{26}$$

To derive the second equation, we first use (22) and rewrite (23) as

$$\sigma p_t + \frac{\kappa p_0}{\alpha_{g0}(1-\sigma\alpha_*\alpha_{g0})}\alpha_{gt} + \left(\frac{\kappa p_0\alpha_{g0z}}{\alpha_{g0}(1-\sigma\alpha_*\alpha_{g0})} + p_{0z}\right)w = 0. \tag{27}$$

Then, by taking the second derivative of (27) with respect to x and using (24) to exclude p, we obtain the second equation:

$$\left(\frac{\kappa p_0 \alpha_{g0z}}{\alpha_{g0}(1-\sigma\alpha_*\alpha_{g0})} + p_{0z}\right) w_{xx} + \frac{\kappa p_0}{\alpha_{g0}(1-\sigma\alpha_*\alpha_{g0})}\alpha_{gtxx}$$
$$+\sigma\rho_0\left[w_{ztt} - \frac{\sigma\alpha_*}{1-\sigma\alpha_*\alpha_{g0}}(\alpha_{gttt} + \alpha_{g0z}w_{tt})\right] = 0. \tag{28}$$

We now use the Boussinesq approximation, so that $\sigma \ll 1$. In this case (26) becomes

$$\frac{\partial^2}{\partial t^2}(w_{xx} + w_{zz}) - \left(\frac{1}{\sigma}\frac{\rho_{0z}}{\rho_0} + \alpha_*\alpha_{g0z}\right) w_{xx} - \alpha_*\alpha_{gtxx} = 0. \tag{29}$$

Next from (28) we obtain, likewise in the Boussinesq approximation,

$$\frac{\kappa p_0}{\alpha_{g0}}\alpha_{gtxx} + \left(\kappa p_0 \frac{\alpha_{g0z}}{\alpha_{g0}} + p_{0z}\right) w_{xx} = 0. \tag{30}$$

Substituting (30) into (29), we finally get a single equation for the internal wave mode,

$$\frac{\partial^2}{\partial t^2}(w_{xx} + w_{zz}) + N_{eff}^2(z) w_{xx} = 0, \tag{31}$$

where the value of the buoyancy frequency in the fluid should be replaced by the effective buoyancy frequency

$$N_{eff}^2(z) = -\frac{1}{\sigma}\frac{\rho_{0z}}{\rho_0} + \frac{\alpha_*\alpha_{g0}}{\kappa}\frac{p_{0z}}{p_0}. \tag{32}$$

Note that equation (31) can be obtained by dropping the $O(\sigma)$ terms in all equations (19) - (23) except (21) from the outset, similar to the use of the Boussinesq approximation in the absence of any bubbles.

Taking into account that $\rho_0 = \rho_l(1-\sigma\alpha_*\alpha_{g0})$ and $p_{0z} = -\rho_0$, (32) yields

$$N_{eff}^2(z) = -\frac{1}{\sigma}\frac{\rho_{l0z}}{\rho_0} - \alpha_*\alpha_{g0z} - \frac{\alpha_*\alpha_{g0}}{\kappa}\frac{\rho_0}{p_0} + O(\sigma).$$

Returning to the dimensional variables, we obtain, in the Boussinesq approximation,

$$N_{eff}^2(z) = -g\frac{\rho_{l0z}}{\rho_{l0}} + g\alpha_{g0z} - \frac{g^2\rho_0\alpha_{g0}}{\kappa p_0}$$
$$= N_l^2 + g\alpha_{g0z} - \frac{g^2\rho_0\alpha_{g0}}{\kappa p_0}. \tag{33}$$

Here $N_l^2 = -g\rho_{l0z}/\rho_{l0}$ is the value of the buoyancy frequency in the pure fluid. The formula (33) reflects two physical factors affecting the buoyancy frequency in the mixture: the effective stratification due to the bubbles adds to the effect of the stratification in the fluid, while the compressibility of the mixture due to the bubbles reduces the buoyancy frequency. Considering the typical oceanic conditions, let the buoyancy frequency of the pure fluid be in the range $N_l = 10^{-3}$ to 10^{-2} s^{-1}. Let us assume an exponential decay of the void fraction, so that $\alpha_{g0z} = \gamma\alpha_{g0}$ where $\gamma \approx 0.5 - 0.9$ m^{-1} (e.g., Buckingham 1997). Also, $\rho_0 = 10^3$ kg m^{-3}, $p_0 = 10^5$ Pa, $\kappa = 1.4, g = 9.8$ m s^{-2}. Then, we estimate the second term in (33) to be $O(10 \cdot \alpha_{g0})$, while the last term is $O(\alpha_{g0})$. Thus, we conclude, that there can be an anomalous high value of the effective buoyancy frequency in the upper mixed layer due to the depth-dependent distributions of bubbles, compared to the situation without the bubbles. Typically if the void fraction α_{g0} is in the range 10^{-5} to 10^{-3}, then the corrections to N_l are comparable with N_l itself. Also, let us note that for typical oceanic conditions, the correction to the buoyancy frequency due to the bubble stratification is about ten times bigger than the correction due to the compressibility of the bubble mixture.

4 Normal modes

4.1 Baroclinic modes

In the present Boussinesq approximation equation (31) is supplemented by the usual surface and bottom boundary conditions:

$$w|_{z=0} = 0, \quad w|_{z=-H} = 0.$$

That is, as well as a rigid flat bottom, the free surface is approximated by a rigid lid in the usual way.

We look for solutions of (31) in the form

$$w = \phi(z) \exp[i(kx - \omega t)] + c.c.,$$

which leads to the Sturm-Liouville problem

$$\phi'' + \frac{k^2(N_{eff}^2(z) - \omega^2)}{\omega^2}\phi = 0\,, \tag{34}$$

where

$$\phi|_{z=0} = 0, \quad \phi|_{z=-H} = 0.$$

It is well known (e.g., Miropol'sky 2001) that this boundary value problem typically has countably many solutions (modes), characterized by their dispersion curves:

$$\omega = \omega_n(k), \quad n = 1, 2, 3, ...$$

Each such curve is a monotonic function of k, $0 < \omega_n(k) < \mu$, and $\lim_{k->\infty} \omega_n = \mu$, where μ is the maximum of $N_{eff}(z)$ on the interval $[-H, 0]$.

Let us assume that the buoyancy frequency of the pure fluid is a constant, $N_l = const.$ Then, the density of the fluid is given by

$$\rho_{l0} = \rho_a e^{-\frac{N_l^2}{g}z},$$

where ρ_a is the density at the free surface. For oceanic conditions, the void fraction either decays exponentially, or follows the inverse square law (see the Introduction). Here, we assume an exponential dependance $\alpha_{g0} = \alpha_a e^{\gamma z}$, with $\gamma \approx 0.5 - 0.9$ m^{-1} (Buckingham 1997) and α_a is the value of void fraction close to the free surface. Then, the density of the mixture is

$$\rho_0 = \rho_a e^{-\frac{N_l^2}{g}z}\left(1 - \alpha_a e^{\gamma z}\right).$$

The pressure in the mixture is given by

$$p_0 = p_a + \frac{\rho_a g^2}{N_l^2}\left(e^{-\frac{N_l^2}{g}z} - 1\right) + \frac{\alpha_a \rho_a g^2}{\gamma g - N_l^2}\left(e^{(\gamma - \frac{N_l^2}{g})z} - 1\right),$$

where p_a is the atmospheric pressure.

This leads to the following expression for the effective buoyancy frequency:

$$N_{eff}^2(z) = N_l^2 + N_g^2(z) - N_c^2(z), \tag{35}$$

$$\text{where} \quad N_g^2(z) = g\gamma\alpha_a e^{\gamma z}, \quad N_c^2(z) = \varepsilon g\gamma\alpha_a \tilde{N}_c^2(z), \tag{36}$$

$$\tilde{N}_c^2(z) = \frac{e^{(\gamma - \frac{N_l^2}{g})z}(1 - \alpha_a e^{\gamma z})}{1 + \frac{\rho_a g^2}{p_a N_l^2}\left(e^{-\frac{N_l^2}{g}z} - 1\right) + \frac{\alpha_a \rho_a g^2}{p_a(\gamma g - N_l^2)}\left(e^{(\gamma - \frac{N_l^2}{g})z} - 1\right)}, \quad \varepsilon = \frac{\rho_a g}{\gamma\kappa p_a}. \tag{37}$$

Here, $N_g^2(z)$ denotes the contribution due to the effective stratification in the presence of bubbles, and $N_c^2(z)$ denotes the contribution due to the compressibility of the mixture.

For the typical oceanic conditions, $\rho_a = 10^3$ kg m^{-3}, $g = 9.8$ m s^{-2}, $\gamma = 0.5 - 0.9$ m^{-1}, $\kappa = 1.4$, $p_a = 10^5$ N m^{-2}, which leads to $\varepsilon \approx 0.08 - 0.14$. Thus, the equation (34) takes the form

$$\phi'' + \frac{k^2(N_l^2 + g\gamma\alpha_a e^{\gamma z} - \omega^2)}{\omega^2}\phi = \varepsilon\frac{k^2}{\omega^2}\, g\gamma\alpha_a\tilde{N}_c^2(z)\phi, \tag{38}$$

where the term on the right-hand side can be treated as a perturbation of the main terms on the left-hand side.

We are now looking for solutions of (38) in the form:

$$\phi = \phi_0 + \varepsilon\tilde{\phi} + O(\varepsilon^2), \quad \omega^2 = \omega_0^2 + \varepsilon\lambda + O(\varepsilon^2),$$

which to the leading order yields

$$\phi_0'' + \frac{k^2(N_l^2 + g\gamma\alpha_a e^{\gamma z} - \omega_0^2)}{\omega_0^2}\phi_0 = 0, \tag{39}$$
$$\phi_0|_{z=0} = 0, \quad \phi_0|_{z=-H} = 0.$$

Let us make a change of variable:

$$\tilde{z} = 2\sqrt{a}e^{\gamma z/2},$$

where $a = g\alpha_a k^2/\gamma\omega_0^2$. Then, the unperturbed equation (39) assumes the form of the Bessel equation (e.g., Abramowitz and Stegun 1979)

$$\tilde{z}^2\phi_0'' + \tilde{z}\phi_0' + (\tilde{z}^2 - \nu^2)\phi_0 = 0, \quad \nu^2 = \frac{4k^2(\omega_0^2 - N_l^2)}{\gamma^2\omega_0^2}. \tag{40}$$

This equation is supplemented by the boundary conditions

$$\phi_0|_{\tilde{z}=2\sqrt{a}} = 0, \quad \phi_0|_{\tilde{z}=2\sqrt{a}e^{-\gamma H/2}} = 0. \tag{41}$$

The general solution of (40) is given by

$$\phi_0(\tilde{z}) = C_1 J_\nu(\tilde{z}) + C_2 Y_\nu(\tilde{z}), \tag{42}$$

where J_ν and Y_ν are Bessel functions of the first and second kind. (Note, that for $\omega_0 < N_l$ the order ν of the Bessel functions will be purely imaginary. For $N_l < \omega_0 < \mu$, the parameter ν and the Bessel functions of the corresponding order are real.)

The boundary conditions (41) imply that the dispersion curves $\omega_0 = \omega_{0n}(k)$ $(n = 1, 2, 3, ...)$ for the internal modes are given by the roots of the following equation:

$$J_\nu(2\sqrt{a})Y_\nu(2\sqrt{a}e^{-\gamma H/2}) - Y_\nu(2\sqrt{a})J_\nu(2\sqrt{a}e^{-\gamma H/2}) = 0. \quad (43)$$

The non-normalized real-valued modal functions of the problem (39) can be written in the form

$$\phi_{0n}(z) = Y_{\nu_n}(2\sqrt{a_n})J_{\nu_n}(2\sqrt{a_n}e^{\gamma z/2}) - J_{\nu_n}(2\sqrt{a_n})Y_{\nu_n}(2\sqrt{a_n}e^{\gamma z/2}) + c.c. \ (n = 1, 2, 3, ...) \quad (44)$$

Before we proceed, let us mention that in the limit to the pure fluid situation, i.e. $\alpha_a \to 0$, the dispersion relation (43) reduces to the usual dispersion relation for the internal waves

$$\omega^2 = \frac{k^2 N_l^2}{k^2 + (\frac{n\pi}{H})^2}, \quad (45)$$

with $n = 1, 2, 3....$ Indeed, for a small fixed value of α_a and fixed values of k and ω, the parameter $a = g\alpha_a k^2/\gamma\omega^2$ is also small. Then, using the standard expansions of the Bessel functions in the vicinity of zero (see the Appendix) and considering the limit $\alpha_a \to 0$, we obtain

$$\cosh\frac{\gamma\nu H}{2} = 0. \quad (46)$$

Here, $\gamma\nu/2 = k\sqrt{\omega^2 - N_l^2}/\omega$. For the real values of this parameter, equation (46) has no solutions. Therefore, one has to consider the imaginary values,

$$\frac{k}{\omega}\sqrt{\omega^2 - N_l^2} = il, \quad (47)$$

which leads to the equation $\cos lH = 0$ instead of (46). This equation has countably many solutions $lH = n\pi$, for the integer values of n. Then, substituting these values into the equation (47), one obtains (45).

Let us now consider first the opposite case when the stratification is primarily due to the bubbles: we assume that $N_l = 0$, i.e. $\rho_{l0} = \rho_a = const$. This leads to the following expression for the effective buoyancy frequency:

$$N_{eff}^2(z) = g\gamma\alpha_a e^{\gamma z}[1 - \varepsilon n^2(z)], \quad (48)$$

where

$$n^2(z) = \frac{1 - \alpha_a e^{\gamma z}}{1 - \frac{\rho_a g}{p_a}z + \frac{\alpha_a \rho_a g}{\gamma p_a}(e^{\gamma z} - 1)} = \frac{p_a}{p_a - \rho_a g z} + O(\alpha_a).$$

Here, we consider again just the leading order problem ($\varepsilon = 0$). The compressibility effect will be estimated later.

In this case, the order ν of the Bessel functions in (44) is real. The roots of the dispersion equation (43) are real and simple (e.g., Tranter 1968). An asymptotic formula can be written down for the high order zeros of this equation (e.g., Abramowitz and Stegun 1979). However, only the first modes are interesting from a physical point of view. Below we show the numerically found from (43) dispersion curves for the first three modes, for a realistic set of parameters: $H = 100$ m, $\gamma = 0.5$ m^{-1}, $\alpha_a = 0.001$ (figure 1).

The modal functions corresponding to the dispersion curves shown in figure 1 are plotted in figure 2, for two different values of the wavenumber k: $k = 0.01$ m^{-1} and $k = 0.12$ m^{-1}. Thus, a depth-dependent distribution of bubbles leads to the existence of internal modes in an otherwise homogeneous fluid. It is interesting to note that although the void fraction of bubbles decays rather rapidly with depth, the modes shown in figure 2

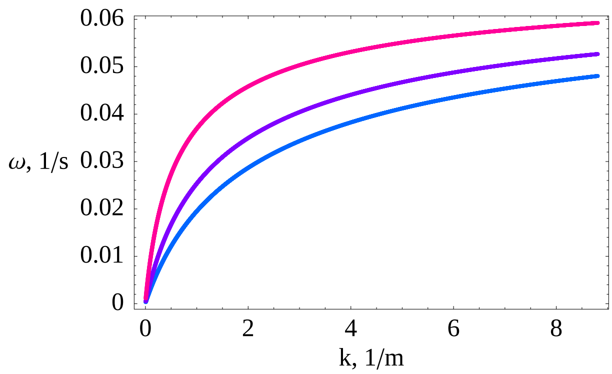

Figure 1: Three first dispersion curves for $H = 100$ m, $\gamma = 0.5$ m^{-1}, $\alpha_a = 0.001$.

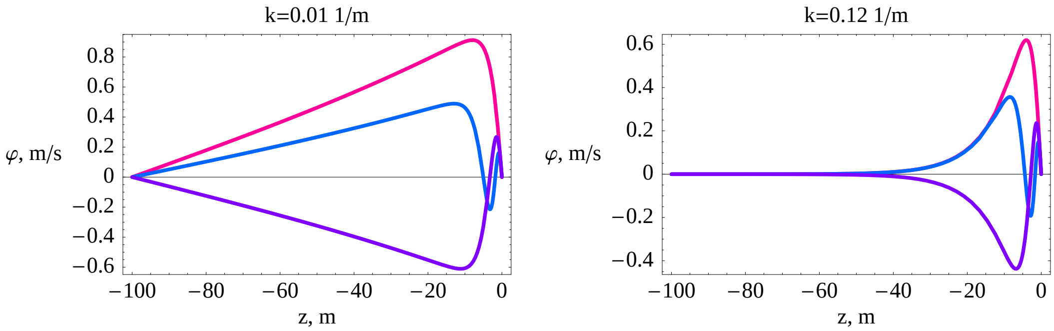

Figure 2: Three first modal functions for $H = 100$ m, $\gamma = 0.5$ m^{-1}, $\alpha_a = 0.001$.

are not trapped in the very upper part of the waveguide. Instead, they are still present at a considerable depth. For the cases shown, this is because the waves are long compared to the depth of the bubble layer ($k/\gamma = 0.02, 0.24$ respectively), although they are not long waves compared to the total depth ($kH = 1, 12$ respectively). Only very short internal waves, with $k \geq \gamma^{-1}$, will have modes trapped within the bubble layer. We also examined the case when $H = 500$ m, with all the other parameters unchanged. The dispersion curves are qualitatively unchanged, with some small quantitative differences arising only for very small values of k. Since now $kH = 5, 60$ respectively, the modes do not "feel" the bottom, and instead decay in the deeper water as k^{-1}. For the case of $k = 0.12$ there is a no observable change in the modal structure; for the case $k = 0.01$ while there is no observable qualitative change in the modal structure in the bubble layer, there is a minor qualitative difference in the modal structure in the deeper water, where now the decay is exponential rather than the near-linear decay shown in figure 2.

Let us next assume that there is a uniform background fluid stratification $N_l = const$. In this case, we have two weakly connected waveguides: the main fluid waveguide due to the stratification of the fluid, and the additional bubble waveguide due to the depth-dependent distribution of bubbles in the upper part of the fluid. As we demonstrated, each of them separately can support wave modes that have their own dispersion curves. In the absence of any coupling, the corresponding dispersion curves would intersect at some finite k. The weak coupling introduced by superimposing the two waveguides induces splitting of the dispersion curves, clearly seen in figure 3 for $N_l = 0.015$ s^{-1} and the same values of other parameters as in figure 1 (that is, $H = 100$ m, $\gamma = 0.5$ m^{-1}, $\alpha_a = 0.001$). Thus, for instance, the first dispersion curve follows the dispersion curve of the main fluid waveguide, but soon after the inflection point where there is a close encounter with the second dispersion curve, it continues as the dispersion curve of the bubble waveguide. An analogous situation holds for the second and third dispersion curves.

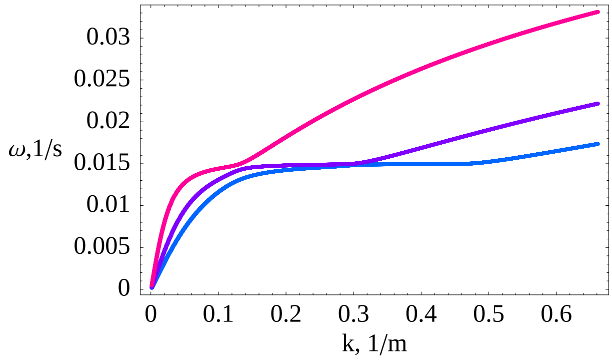

Figure 3: Three first dispersion curves for $H = 100$ m, $\gamma = 0.5$ m^{-1}, $\alpha_a = 0.001$, $N_l = 0.015$ s^{-1}.

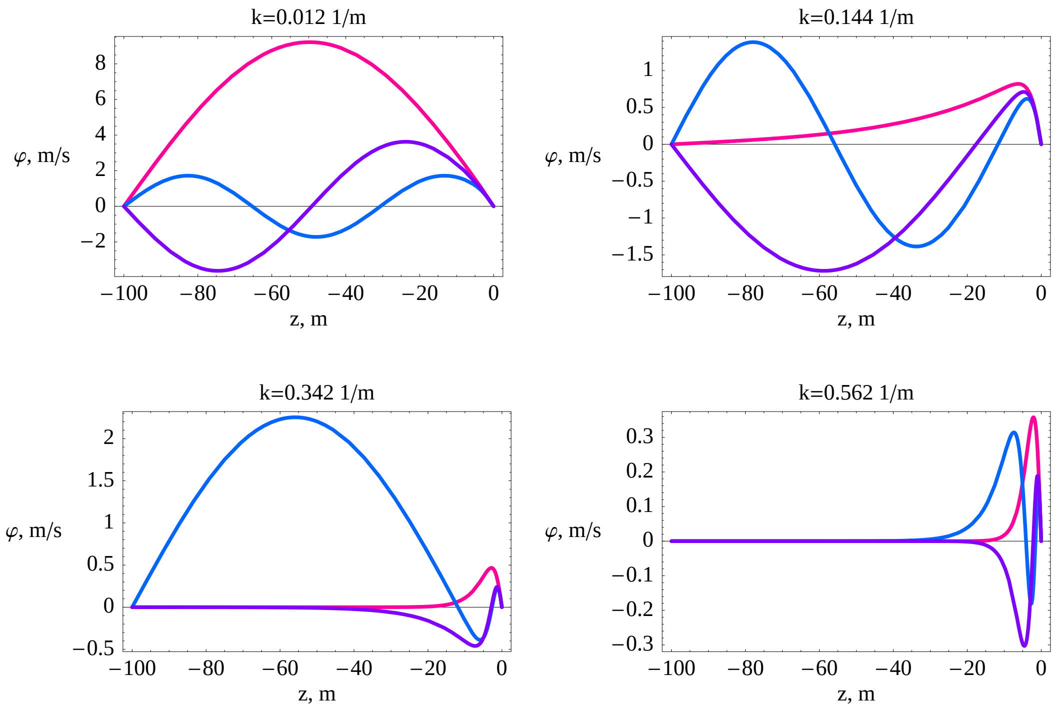

Figure 4: Three first modal functions for $H = 100$ m, $\gamma = 0.5$ m^{-1}, $\alpha_a = 0.001$, $N_l = 0.015$ s^{-1}.

The behaviour of the dispersion curves is reflected in the behaviour of the respective modal functions. The modal functions corresponding to the dispersion curves shown in figure 3 are plotted in figure 4 for four different values of the wavenumber k: $k = 0.012$ m^{-1}, $k = 0.144$ m^{-1}, $k = 0.342$ m^{-1} and $k = 0.562$ m^{-1}. Before the inflection points of the dispersion curves (e.g., $k = 0.012$ m^{-1}), the modes occupy the entire fluid waveguide. Behavior after the inflection points is different. For example, in the vicinity of the inflection point of the first mode ($k = 0.144$ m^{-1}), the first mode becomes trapped in the bubble waveguide, while the second and the third still occupy the entire depth. The same transition occurs for the second and the third modes near the inflection points of the respective dispersion curves ($k = 0.342$ m^{-1} and $k = 0.562$ m^{-1}). For the last value, $k = 0.562$ m^{-1}, all three modes are trapped in the bubble waveguide. Again, we also examined the case when $H = 500$ m, with all the other parameters unchanged, and the dispersion curves are shown in figure 5. They are qualitatively the same as that shown in figure 3, but because the difference between the "internal" mode occupying the whole depth and the "bubble" mode confined to the bubble layer is now more greatly accentuated, the near -"kissing" structure at the inflection points is consequently more prominent. The modal functions have much the same structure in the bubble layer, but in the deeper water now differ from those shown in figure 4; indeed, since the oscillatory structure in the deeper water extends over the whole depth, the modes have essentially the same shape as those shown in figure 4, but are rescaled to fit the whole domain.

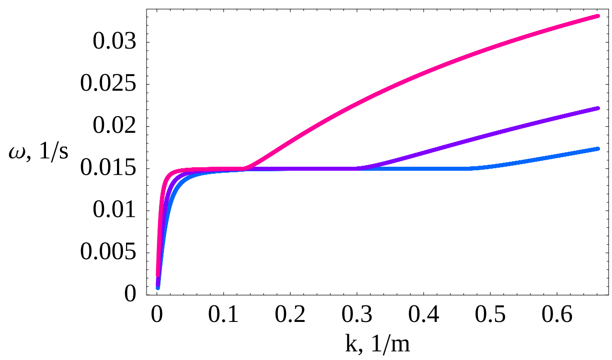

Figure 5: Three first dispersion curves for $H = 500$ m, $\gamma = 0.5$ m^{-1}, $\alpha_a = 0.001$, $N_l = 0.015$ s^{-1}.

We next use a perturbation theory to find corrections to the dispersion relation accounting for the effect of compressibility of the mixture. To find the first correction to (44), one has to solve the following non-homogeneous problem:

$$\tilde{\phi}'' + \frac{k^2(N_l^2 + g\gamma\alpha_a e^{\gamma z} - \omega_0^2)}{\omega_0^2}\tilde{\phi} = \frac{k^2}{\omega_0^2}\left(g\gamma\alpha_a \tilde{N}_c^2(z) + \lambda\frac{N_l^2 + g\gamma\alpha_a e^{\gamma z}}{\omega_0^2}\right)\phi_0, \quad (49)$$
$$\tilde{\phi}|_{z=0} = 0, \quad \tilde{\phi}|_{z=-H} = 0.$$

The solvability condition for this problem requires the orthogonality of the right-hand side of (49) to the solution ϕ_0 of the homogeneous problem, which leads to the following expression for the first correction to the dispersion relation for the modes:

$$\frac{\varepsilon\lambda(k,\omega_0)}{\omega_0^2} = -\varepsilon\frac{g\gamma\alpha_a\int_{-H}^{0}\tilde{N}_c^2(z)\phi_0^2(z)dz}{\int_{-H}^{0}(N_l^2 + g\gamma\alpha_a e^{\gamma z})\phi_0^2(z)dz}, \quad \omega_0 = \omega_{n0}(k), \quad n = 1, 2, 3, ... \quad (50)$$

From (37), it is readily shown that

$$\frac{g\gamma\alpha_a\tilde{N}_c^2(z)}{N_l^2 + g\gamma\alpha_a e^{\gamma z}} < 1.$$

Then, taking into account that both integrands in (50) are nonnegative in the interval $[-H, 0]$, we deduce that

$$\left|\frac{\varepsilon\lambda(k,\omega_0)}{\omega_0^2}\right| < \varepsilon.$$

Thus, for a fixed k, compressibility results in decreasing the frequency compared to ω_0, but the value of the correction to the frequency due to this effect is small (in typical oceanic conditions, $\varepsilon \approx 0.08 - 0.14$, see above). Hence, it seems that compressibility effects can usually be ignored.

4.2 Barotropic mode

For completeness, we now consider the barotropic mode, and so we must replace the rigid-lid condition at the upper boundary with the (linearized) free-surface boundary conditions,

$$w|_{z=0} = \eta_t, \tag{51}$$

$$p|_{z=0} = g\rho_0(0)\eta \tag{52}$$

where η is the free surface elevation, and the second condition arises by linearization of the condition that the full pressure field $p_0(z) + p$ is a constant on the free surface $z = \eta$. Then, using (24), in the Boussinesq approximation (i.e., neglecting terms of relative order $O(\sigma)$), and eliminating p from the boundary conditions (51), (52), we get

$$w_{ztt} - gw_{xx}|_{z=0} = 0. \tag{53}$$

We can now consider the same setting as in the previous section and again look for solutions of (31) in the form of normal modes

$$w = \phi(z)\exp[i(kx - \omega t)] + c.c.,$$

supplemented by the boundary condition (53) at the free surface, and the boundary condition that $w|_{z=-H}$ at the rigid bottom. In the following we ignore the effect of compressibility of the mixture and concentrate on the solution of the leading order problem in (38) ($\varepsilon = 0$), using (42). Thus we now find that the dispersion curves for the normal modes are given by the roots of the following equation,

$$\frac{J_\nu(2\sqrt{a})Y_\nu(2\sqrt{a}e^{-\gamma H/2}) - Y_\nu(2\sqrt{a})J_\nu(2\sqrt{a}e^{-\gamma H/2})}{J'_\nu(2\sqrt{a})Y_\nu(2\sqrt{a}e^{-\gamma H/2}) - Y'_\nu(2\sqrt{a})J_\nu(2\sqrt{a}e^{-\gamma H/2})} = \frac{\alpha_a}{\sqrt{a}}, \tag{54}$$

where the prime denotes differentiation with respect to the argument of a function, and we use

$$J'_\nu(z) = \frac{1}{2}[J_{\nu-1}(z) - J_{\nu+1}(z)], \quad Y'_\nu(z) = \frac{1}{2}[Y_{\nu-1}(z) - Y_{\nu+1}(z)]$$

(e.g., Tranter 1968).

The corresponding modal functions assume the (non-normalized) form

$$\begin{aligned}\phi_{0n}(z) \quad = \quad & Y_{\nu_n}(2\sqrt{a_n}e^{-\frac{\gamma H}{2}})J_{\nu_n}(2\sqrt{a_n}e^{\gamma z/2}) - J_{\nu_n}(2\sqrt{a_n}e^{-\frac{\gamma H}{2}})Y_{\nu_n}(2\sqrt{a_n}e^{\gamma z/2}) \\ & +c.c. \; (n = 1, 2, 3, ...)\end{aligned} \tag{55}$$

First, let us note that in the limit of a pure homogeneous fluid, i.e. $\alpha_a \to 0, N_l = 0$, the dispersion relation (54) yields the well-known dispersion relation for the surface waves:

$$\omega^2 = gk\tanh kH. \tag{56}$$

Indeed, since $N_l = 0$, the parameter $\nu = 2k/\gamma$ is real. We then consider a small value of α_a for fixed values of k and ω; the parameter $a = g\alpha_a k^2/\gamma\omega^2$ is also small. Using the

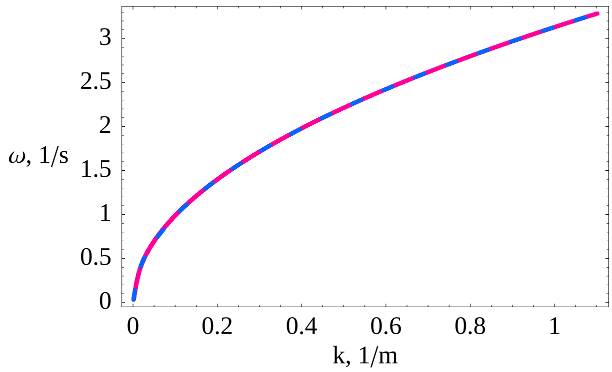

Figure 6: Dispersion curve for the barotropic mode for $H = 100$ m, $\gamma = 0.5$ m^{-1}, $\alpha_a = 0.001$, $N_l = 0.015$ s^{-1} (solid line - in the mixture, dashed line - in the pure homogeneous liquid; the curves coincide).

standard expansions of Bessel functions in the vicinity of zero (see the Appendix), we obtain the following limit

$$\tanh \frac{\gamma \nu H}{2} = \frac{\nu \alpha_a}{2a},$$

which after the substitution of the expressions for ν and a yields (56).

The dispersion curves and modal functions for the baroclinic modes computed in accordance with the dispersion relation (54) and the formula (55) respectively are essentially the same as in the the rigid-lid approximation (43) and, therefore, are not shown here. However, in contrast to the dispersion relation (43), the new dispersion relation (54) has one additional root, which corresponds to the barotropic mode. The corresponding dispersion curve is shown in figure 6, together with the dispersion curve (56) in the homogeneous fluid in the absence of any bubbles (shown by the dashed line). We see that the curves almost coincide. Similarly we find that the modal functions are virtually indistinguishable. Thus, unlike internal waves, bubble distributions (as well as the basic fluid stratification) have virtually no effect on surface waves, as expected.

5 Concluding remarks

In this paper we have considered how the presence of bubbles in the upper part of the ocean affects the normal modes, with an emphasis on the internal wave modes. Restricting attention to the low-frequency case, and then using a quasistatic approximation for the bubbles, has allowed us to formulate an analytical model suitable for polydisperse mixtures (i.e. distributions of bubbles). Asymptotic analysis of our model has shown that, to the leading order in the Boussinesq approximation, the normal modes are described by the usual model equation, but with an effective buoyancy frequency, which takes account of the near-surface bubble distribution. We then considered the important case of a uniform fluid stratification with a near-surface, exponentially-decaying void fraction for the bubbles, for which we obtained an explicit description of the normal modes for both the classical rigid-lid formulation, appropriate for internal waves, and also for the free-surface formulation of the boundary-value normal mode problem. Considering the typical oceanic situation, we have shown that bubbles, when present, change the properties of the oceanic waveguide, resulting in the appearance of an additional bubble waveguide in the upper part of the ocean. Somewhat counter-intuitively, the corresponding modes are usually not trapped in the first few meters of the waveguide depth. Instead, their presence can be felt at a considerable depth.

When applying our results to a typical oceanic situation, it is necessary to re-evaluate some of the simplifying assumptions made in the basic model development described in Section 2. In particular, we have assumed that the bubbles move with the velocity of the fluid flow, whereas in reality the bubbles can move relative to the surrounding fluid. Also we have ignored the dissolution of bubbles due to gas diffusion. Concerning the relative motion of the bubbles, the most important effect is due to their buoyancy, which allows them to potentially rise to the surface. Estimates of the bubble rise velocity have been obtained by Thorpe (1982) (see also Garrett et al. 2000 and Buckingham 1997). For small oceanic bubbles the rise speed is approximately given by

$$w_b = \frac{2}{9} \cdot \frac{ga^2}{\nu} \left(\sqrt{y^2 + 2y} - y \right), \quad y = 10.82 \cdot \frac{\nu^2}{ga^3},$$

where a is the radius ($a \leq 180\ \mu$m), $\nu = 10^{-6}$ m^2 s^{-1} is the kinematic viscosity, $g = 9.8$ m s^{-2} is gravity. (Note that w_b tends to $2ga^2/9\nu$ as a tends to zero.) As mentioned in the Introduction, bubbles with radii of approximately $50 - 100\ \mu$m contribute most to the total void fraction, and so a reasonable estimate for w_b would be $0.005 - 0.016$ m s^{-1}. Thus we would expect our present model to be valid for internal wave modes whose vertical velocities are greater than w_b. But this is probably an over-estimate, since, according to Thorpe (1982), the tendency of bubbles to rise is balanced by turbulent diffusion. Thus, generally turbulence helps to maintain the quasi-static bubble distribution.

Further, our results may also carry over to the case when rising bubbles are replaced by newly injected ones, so that the average depth-dependent distribution of bubbles is quasi-stationary. For the quasi-static processes considered here this situation holds, because a "newborn" individual bubble immediately acquires the phase and amplitude corresponding to the local pressure in the internal wave as prescribed by the equation of state. Note that for non-quasistatic models in which transient processes and resonances are taken into account, the situation will be much more complicated. Indeed, different "newborn" bubbles start with different phases with respect to the wave, and their motion (consisting of forced and free oscillations) may give a more complex contribution to the wave, including resonant cases. Such effects are known in electrodynamics and acoustics (e.g., Naugolnykh and Ostrovsky 1998). Fortunately, for internal waves the quasistatic approximation is almost always justified.

For the dissolution of bubbles, we will use Thorpe's formula

$$a = a_0 - Dt,$$

where $D = 2 \cdot 10^{-9}$ m^2 s^{-1} is the dissolution rate, assumed to be independent of radius (Thorpe 1982). Bubbles with a radii of approximately $50 - 100\ \mu$m dissolve in a time of order $(2.5 - 5) \cdot 10^4$ s, which usually exceeds the period of the internal waves in question. These preliminary estimates invite further detailed consideration of the aforementioned issues.

Finally, we would like to note that, strictly speaking, the present model has only limited applicability to the description of the *surface* waves in the situation considered in this paper. Indeed, it would be more appropriate to consider large-amplitude breaking surface waves (which are highly nonlinear), which inject bubbles into the water (some results in this direction were obtained in a recent paper by Peregrine et al. 2004). Such waves have a large fraction of air in the mixture and foam on the top, and our model is not applicable in this situation. However, we expect our description to be applicable to small amplitude surface waves propagating immediately after the cessation of breaking of large amplitude surface waves.

6 Acknowledgments

We are grateful to Ya. V. Kurylev for clarifying discussions. We thank the London Mathematical Society for their financial support of LAO to Loughborough making this collaboration possible.

7 Appendix

In the Appendix, we list expansions of the Bessel functions of the first and second kind in the vicinity of zero (e.g., Abramowitz and Stegun, 1972), used in sections 4.1 and 4.2.

We restrict our considerations to the generic case when ν is a complex number and not an integer. Then, for small $|z|$ (in our case z is real and positive) the Bessel function of the first kind can be expanded as

$$J_\nu(z) = z^\nu \left(\frac{2^{-\nu}}{\Gamma(\nu+1)} + O(z^2) \right).$$

The Bessel function of the second kind, $Y_\nu(z)$ (also, $N_\nu(z)$) is defined as

$$Y_\nu(z) = \frac{1}{\sin \nu\pi} [J_\nu(z) \cos \nu\pi - J_{-\nu}(z)],$$

and has the following expansion

$$Y_\nu(z) = z^\nu \left(-\frac{2^{-\nu} \cos \nu\pi \Gamma(-\nu)}{\pi} + O(z^2) \right) + z^{-\nu} \left(-\frac{2^\nu \Gamma(\nu)}{\pi} + O(z^2) \right),$$

In the formulae above, $\Gamma(...)$ is the Gamma function.

References

[1] Abramowitz, M. and I.A. Stegun ed., 1972: Handbook of mathematical functions. Wiley-Interscience, 830 pp.

[2] Buckingham, M.J., 1997: Sound speed and void fraction profiles in the sea surface bubble layer. *Applied Acoustics* **51**, 3, 225-250.

[3] Farmer, D.M. and D.D. Lemon, 1984: The influence of bubbles on ambient noise in the ocean at high wind speeds. *J. Phys. Oceanogr.* **14**, 1762-1778.

[4] Farmer, D.M. and S. Vagle, 1989: Wavequide propagation of ambient sound in the ocean-surface bubble layer. *J. Acoust. Soc. Am.* **86**, 1897-1908.

[5] Farmer, D.M., Vagle, S., and M. Li, 1999: Wave breaking, turbulence and bubble distributions in the ocean surface layer. Proceedings, *The wind-driven air-sea interface*, M.L. Banner, Ed., The University of New South Wales, 187-192.

[6] Gill, A.E., 1982: Atmosphere-ocean dynamics. Academic, 662 pp.

[7] Grimshaw, R.H.J., and K.R. Khusnutdinova, 2004a: The effect of bubbles on internal waves. *J. Phys. Oceanogr.* **34**, 477-489.

[8] Grimshaw, R.H.J., and K.R. Khusnutdinova, 2004b: Internal waves in a three-layer bubbly waveguide. *Deep-Sea Research II* **51**, 2905-2917.

[9] Iordansky, S.V., 1960: Equations of motion of liquid containing gas bubbles. *Zh. Prikl. Mekh. Tekh. Fiz.* **3**, 102-110 (in Russian).

[10] Kogarko, B.S., 1961: On the model of cavitating liquid. *Dokl. AN SSSR* **137**, 1331-1333 (in Russian).

[11] LeBlond P.H. and L.A. Mysak, 1978: Waves in the ocean. Elsevier, 602 pp.

[12] Miropol'sky, Yu. Z., 2001: Dynamics of internal gravity waves in the ocean. Kluwer, 406 pp.

[13] Naugolnykh, K., L. Ostrovsky, 1998: Nonlinear wave processes in acoustics. Cambridge University Press, 298 pp.

[14] Nigmatulin, R.I., 1991: Dynamics of multiphase media, Vol.1 & 2. Hemisphere, 507 & 371 pp.

[15] Peregrine, D.H., H. Bredmose, G. Bullock, C. Obrhai, G. Müller and G. Wolters, 2004: Water wave impact on walls and the role of air. Proceedings, *29th Internat. Conf. on Coastal Engineering*, Lisbon, J. Mck. Smith, Ed., World Sci. **4**, 4005-4017.

[16] Terrill, E.J. and W.K. Melville, 1999: Field measurements of bubble size distributions in the upper mixed layer. Proceedings,*The wind-driven air-sea interface*, M.L. Banner, Ed., The University of New South Wales, 247-255.

[17] Thorpe, S.A., 1982: On the clouds of bubbles formed by breaking wind-waves in deep water, and their role in air-sea gas transfer. *Phil. Trans. R. Soc. Lond. A* **304**, 155-210.

[18] Thorpe, S.A., 1984: A model of the turbulent diffusion of bubbles below the sea surface. *J. Phys. Oceanogr.* **14**, 841-853.

[19] Tranter, C.J., 1968: Bessel functions with some physical applications. The English Universitites Press, 148 pp.

[20] van Wijngaarden, L., 1968: On the equations of motion for mixtures of liquid and gas bubbles. *J. Fluid Mech.* **33**, 465-474.

[21] Zedel, L. and D. Farmer, 1991: Organized structures in subsurface bubble clouds: Langmuir circulation in the open ocean, *J. of Geophys. Res.* **96**, C5, 8889-8900.